

## Phase Transition in the $\nu = 2$ Bilayer Quantum Hall State

A. Sawada,<sup>1</sup> Z. F. Ezawa,<sup>1</sup> H. Ohno,<sup>2</sup> Y. Horikoshi,<sup>3</sup> Y. Ohno,<sup>2</sup> S. Kishimoto,<sup>2</sup> F. Matsukura,<sup>2</sup>  
M. Yasumoto,<sup>1</sup> and A. Urayama<sup>1</sup>

<sup>1</sup>*Department of Physics, Tohoku University, Sendai 980-8578, Japan*

<sup>2</sup>*Research Institute of Electrical Communication, Tohoku University, Sendai 980-8577, Japan*

<sup>3</sup>*School of Science and Engineering, Waseda University, Tokyo 169-8555, Japan*

(Received 29 December 1997)

The width of the Hall plateau and the activation energy were measured in the bilayer quantum Hall state at filling factors  $\nu = 2, 1$ , and  $2/3$  by changing the total electron density and the density ratio in the two quantum wells. Their behaviors are remarkably different. The  $\nu = 1$  state is found to be stable over all measured range of the density difference. The  $\nu = 2/3$  state is stable only around the balanced point. The  $\nu = 2$  state shows a phase transition between these two types of states as the electron density is changed. [S0031-9007(98)06109-2]

PACS numbers: 73.40.Hm, 72.20.My, 73.20.Dx, 73.40.Kp

Electron systems in confined geometries exhibit a rich variety of physical properties due to the interaction effects in reduced dimensions. One of the most interesting phenomena is the quantum Hall (QH) effect in the planar electron system. In particular, the QH effect in double quantum wells has recently attracted much attention [1,2], where the structure introduces additional degrees of freedom in the third direction. Various bilayer QH states are realized [3,4] by controlling system parameters such as the strengths of the interlayer and intralayer Coulomb interaction, the tunneling interaction, and the Zeeman effect. A good example is the  $\nu = 1/2$  state [4] for which there is no counterpart in the monolayer system. Here,  $\nu$  is the total filling factor. It has also been pointed out [5,6] that a novel interlayer quantum coherence (IQC) may develop spontaneously in the  $\nu = 1/m$  state with  $m$  being an odd integer. Murphy *et al.* [7] have reported an anomalous activation energy dependence in the bilayer  $\nu = 1$  QH state on the tilted magnetic field, which is probably one of the signals [8,9] of the IQC. Another unique feature of this IQC [10] is that the QH state is stable at any electron density ratio  $n_f/n_b$ , where  $n_f$  ( $n_b$ ) is the electron density in the front (back) quantum wells.

So far the QH states at  $\nu =$  odd integers have been extensively investigated from the viewpoints of "phase transition" due to the interlayer correlation. The  $\nu = 2$  bilayer QH state has attracted less attention because it has been thought of as a simple "compound" state with  $\nu = 1 + 1$  made of two noninteracting monolayer  $\nu = 1$  states.

In this Letter we report the width of the Hall plateau and the activation energy in three typical bilayer QH states at  $\nu = 2/3, 1$ , and  $2$  by changing the total electron density  $n_t = n_f + n_b$  as well as the density ratio  $n_f/n_b$ . By changing the total density, we can change the ratio of the interlayer to the intralayer Coulomb interactions, which governs the basic nature of the bilayer QH states. Furthermore, the stability of the bilayer QH state, which

is quite sensitive to the density ratio in general, is also tested to clarify the origin of the QH state. The behaviors of these three states have been found to be remarkably different. The  $\nu = 2/3$  state is identified as a compound state with  $\nu = 1/3 + 1/3$ , whereas the  $\nu = 1$  state is found to be the "coherent" state [11]. The  $\nu = 2$  state, on the other hand, shows a phase transition from the compound state to a coherent state as the interlayer Coulomb interaction is enhanced.

The sample was grown by molecular beam epitaxy on a (100)-oriented GaAs substrate and consists of two modulation doped GaAs quantum wells of width  $200 \text{ \AA}$  separated by an  $\text{Al}_{0.3}\text{Ga}_{0.7}\text{As}$  barrier of thickness  $31 \text{ \AA}$ . Carriers are supplied from the two Si delta-doping sheets ( $5 \times 10^{11} \text{ cm}^{-2}$ ), each of which is placed  $750 \text{ \AA}$  away from one of the quantum wells. A Hall-bar mesa was formed by conventional photolithography. Al/Cr Schottky gate electrodes were fabricated on both front and back surfaces of the sample so that the total electron density  $n_t$  and the electron density difference  $n_f - n_b$  can be independently controlled by adjusting the front,  $V_{fg}$ , and the back gate voltage,  $V_{bg}$ .

Measurements were performed with the sample mounted in a mixing chamber of a dilution refrigerator. The magnetic field with maximum  $13.5 \text{ T}$  was applied perpendicular to the electron layers. Standard low-frequency ac lock-in techniques were used with currents less than  $100 \text{ nA}$  to avoid heating effects.

The electron density in each layer is a key parameter in our experiments. We obtained the total electron density  $n_t$  from the Hall resistance at a low magnetic field, and the electron densities in each layer from Fourier transforms of the Shubnikov-de Haas oscillations.

In Fig. 1, the Hall resistance is shown at a various electron density difference  $(n_f - n_b)/n_t$  and at a fixed total electron density of  $1.2 \times 10^{11} \text{ cm}^{-2}$ . Well-developed quantized Hall plateaus are clearly seen at  $\nu = 2/3, 1$ , and  $2$ . The total electron density of this sample

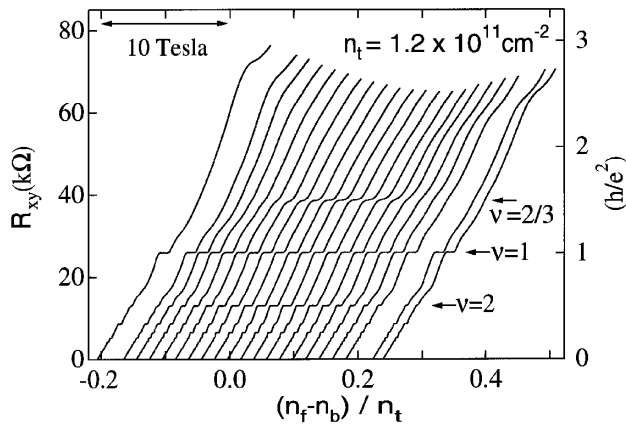


FIG. 1. Hall resistance versus magnetic field at a various density difference at a fixed total electron density  $n_t$ . The origins of the magnetic field axis are shifted in correspondence with the normalized density difference  $(n_f - n_b)/n_t$ .

was  $2.3 \times 10^{11} \text{ cm}^{-2}$  at zero gate voltage, and the mobility was  $3.0 \times 10^5 \text{ cm}^2/\text{Vs}$  at temperature  $T = 30 \text{ mK}$ . The measured tunneling energy gap was  $\Delta_{\text{SAS}} \approx 6.8 \text{ K}$ , which is in good agreement with the value of the self-consistent calculation result  $6.7 \text{ K}$ .

We first concentrate on the width of the Hall plateau, which is a good indicator of the stability of the QH state. We have defined it by the width of the magnetic field within the  $\pm 2.5\%$  range of the Hall resistance after subtracting the classical Hall resistance [10]. The state is stable when the plateau width is wide, and the stability is lost when the width is zero. We later correlate the plateau width to the activation energy.

In Fig. 2 we show the plateau width of the  $\nu = 2/3$ , 1, and 2 QH states as a function of the electron density difference at various total electron densities. The data are slightly out of symmetry with respect to the balanced point. We expect a perfect symmetry in an ideal system.

The plateau width of the  $\nu = 2/3$  state has a peak (*maximum*) at the balanced point. As the total electron density *decreases*, the plateau width at the balanced point decreases. Eventually, the Hall plateau disappears at the total density *less* than  $0.8 \times 10^{11} \text{ cm}^{-2}$ .

The plateau width of the  $\nu = 1$  state has a *minimum* at the balanced point. As the total electron density *increases*, the plateau width at the balanced point decreases. Eventually, the state at the balanced point disappears at the total density *more* than  $1.5 \times 10^{11} \text{ cm}^{-2}$ .

The plateau width of the  $\nu = 2$  state has an intriguing behavior. Around the balanced point, its behavior is quite similar to that of the  $\nu = 2/3$  state. Namely, it has a peak at the balanced point, and as the total density decreases, the plateau width at the balanced point *decreases*. However, its behavior at the off-balanced point ( $|n_f - n_b|/n_t \geq 0.2$ ) is rather similar to that of the  $\nu = 1$  state. The plateau width *increases* as the total density decreases. Furthermore, when the total density

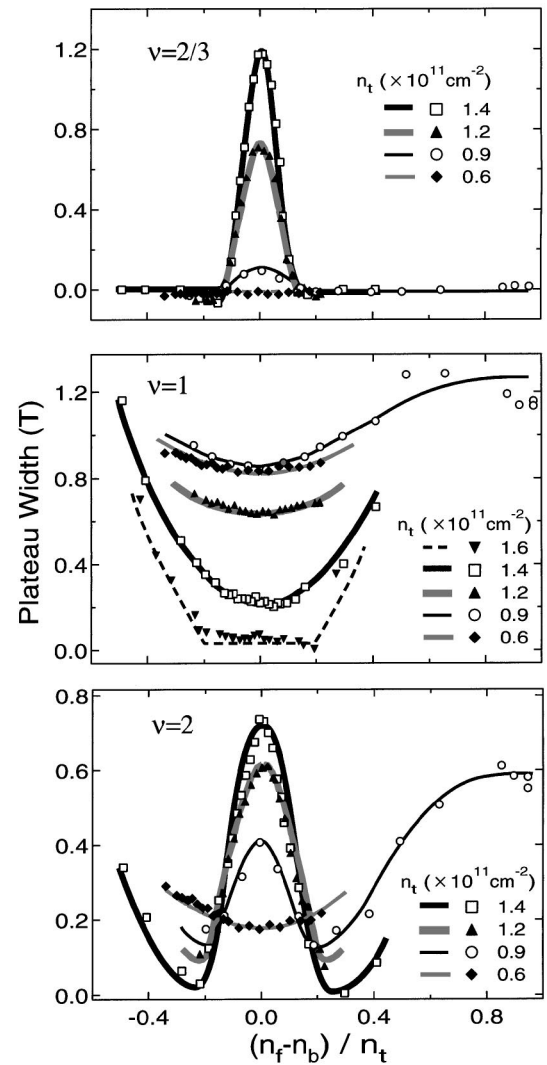


FIG. 2. The Hall-plateau width of the  $\nu = 2/3$ , 1, and 2 states at  $50 \text{ mK}$  as a function of the electron density difference at several fixed total electron densities. The lines are guides to the eye.

is sufficiently small ( $n_t \approx 0.6 \times 10^{11} \text{ cm}^{-2}$ ), the entire behavior now bears a close resemblance to that of the  $\nu = 1$  state.

The data of  $\nu = 2/3$  and 1 clearly show that the two QH states belong to two different types of QH states. Moreover, the data of  $\nu = 2$  indicate that there are two types of  $\nu = 2$  QH state with different properties.

To confirm these observations we measured the activation energy  $\Delta$ , which is derived from the temperature dependence of the magnetoresistance:  $R_{xx} = R_0 \exp(-\Delta/T)$ . As we will see, there is a close connection between the plateau width and the activation energy.

In Fig. 3 we show the activation energy of the  $\nu = 1$  state and the  $\nu = 2$  state as a function of the density difference. As an example of the  $\nu = 1$  state we show the data when the total density is  $1.1 \times 10^{11} \text{ cm}^{-2}$ . The activation energy is  $\Delta = 1 \text{ K}$  at the balanced point

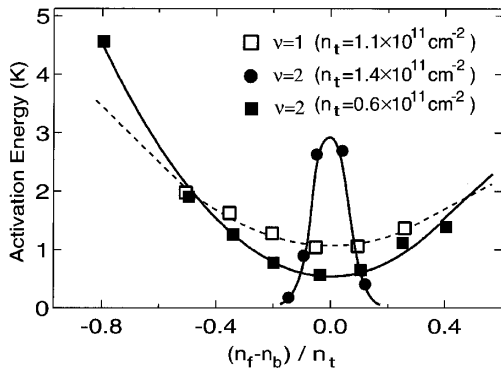


FIG. 3. Activation energy of the  $\nu = 1$  and 2 states as a function of the density difference. The total density is fixed at a constant value. The curves with square data points are fitted by assuming that the activation energy depends on  $(n_f - n_b)^2$ .

and gradually increases to  $\Delta = 4.6$  K at  $(n_f - n_b)/n_t = -0.8$ . For the  $\nu = 2$  state we give the data for two values of the total density. The activation energy at a lower density ( $0.6 \times 10^{11} \text{ cm}^{-2}$ ) is quite similar to that of the  $\nu = 1$  state, while the one at a higher density ( $1.4 \times 10^{11} \text{ cm}^{-2}$ ) has an entirely different property: it has a peak at the balanced point. The overall shapes of the activation energies are in good agreement with the plateau widths seen in Fig. 2.

In Fig. 4 we show the activation energy of the  $\nu = 2/3, 1,$  and 2 QH states at the balanced point as a function of the total electron density. The activation energy of the  $\nu = 2/3$  state shows a weak dependence on the total electron density and vanishes at  $n_t$  less than  $1.1 \times 10^{11} \text{ cm}^{-2}$ . On the other hand, the activation energy of the  $\nu = 1$  state increases as the total electron density decreases and becomes almost constant for  $n_t \leq 1.0 \times 10^{11} \text{ cm}^{-2}$ . The activation energy of the  $\nu = 2$  state linearly depends on the total electron density larger than  $0.9 \times 10^{11} \text{ cm}^{-2}$  and is almost constant when the total density is less.

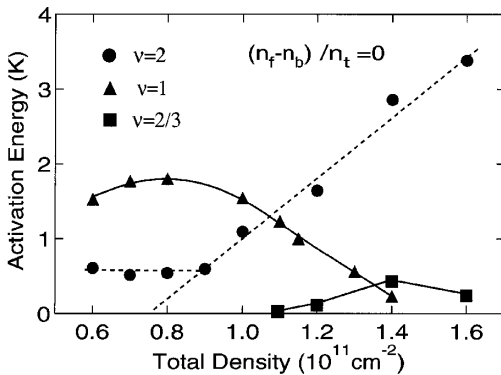


FIG. 4. Activation energy of the  $\nu = 2/3, 1,$  and 2 QH states at the balanced density point, as a function of the total electron density. The lines are guides to the eye.

Let us discuss the peculiar properties of the bilayer QH states observed in our present data. The basic nature of the QH state is governed by the competition between the intralayer and the interlayer Coulomb interactions. Both the Zeeman energy ( $g^* \mu_B B$ ) and the tunneling energy ( $\Delta_{\text{SAS}}$ ) are much smaller than the Coulomb energy ( $e^2/\epsilon \ell_B$ ):  $g^* \mu_B B / (e^2/\epsilon \ell_B) \approx 0.02$  and  $\Delta_{\text{SAS}} / (e^2/\epsilon \ell_B) \approx 0.04$  at  $B = 10$  T in our sample, where  $\ell_B$  is the magnetic length.

We first consider the case where the interlayer Coulomb interaction is negligible with respect to the intralayer Coulomb interaction. In this case the bilayer system decouples into two degenerate independent monolayer systems. Consequently, the compound state becomes stable at  $\nu = 1/m + 1/m$  in the balanced configuration, where all electron spins are polarized. The tunneling interaction is suppressed and the excitation gap may involve mainly spin flips. Even if the interlayer Coulomb interaction is not negligible, the compound state will be realized since the monolayer  $\nu = 1/m$  state is very stable, unless there exists a more stable state at this filling factor.

The  $\nu = 2/3$  state and a part of the  $\nu = 2$  state have clearly all the properties of the compound state. First, they are sharply enhanced in the balanced configuration as in Fig. 2. Second, these states become unstable as the total electron density decreases (or equivalently  $d/\ell_B$  decreases). Third, their activation energy in Fig. 4 behaves as in the monolayer case [12], although this is not so clear for the state at  $\nu = 1/3 + 1/3$ . More quantitatively, by a finite-size calculation [2], the compound state at  $\nu = 1/3 + 1/3$  is known to be unstable when  $d/\ell_B \leq 1.5$ . In our experiment the peak of the  $\nu = 2/3$  state collapses when  $d/\ell_B \leq 2.4$ , where  $d$  is the interlayer separation.

Next, we discuss the case where the interlayer Coulomb interaction is dominant. In general, the bilayer QH state is described by the extended Laughlin wave function [13]  $\Psi_{m_f m_b m}$  at

$$\nu = \frac{m_f + m_b - 2m}{m_f m_b - m^2} \leq 1, \quad (1)$$

where odd integers  $m_f$  and  $m_b$  represent the intralayer electron correlations, while integer  $m$  represents the interlayer correlation induced by the interlayer Coulomb interaction. (The compound state is obtained as a special limit  $m = 0$ .) The density ratio is fixed as

$$\frac{n_f}{n_b} = \frac{m_b - m}{m_f - m}. \quad (2)$$

A strong interlayer correlation supports the coherent state with  $m_f = m_b = m$ , where the density ratio (2) becomes undetermined. It is a characteristic feature of this state [5,8,10] that it is stable at any density ratio and that the IQC may develop spontaneously.

The  $\nu = 1$  state in our data can be identified as this coherent state, since the state continues to exist over all of

the measured range of the density difference, as in Fig. 2. As the total density increases, or equivalently as  $d/\ell_B$  increases, the stability decreases as in Fig. 2, because the interlayer Coulomb interaction becomes weaker. This can also be seen from the behavior of the activation energy in the balanced point in Fig. 4. The state may be regarded sufficiently stable for  $n_t \leq 1.0 \times 10^{11} \text{ cm}^{-2}$ , where the activation energy is almost constant. The QH state breaks down at and above the critical density of  $1.5 \times 10^{11} \text{ cm}^{-2}$  ( $d/\ell_B \approx 2.2$ ), which is in good agreement with the previous experiments [4].

As found in Fig. 2, the coherent state is least stable in the balanced configuration. This is also interpreted as an effect due to an interlayer Coulomb correlation. The activation energy in Fig. 3 is understood if the excitation gap is dominated by the charging energy proportional to  $(n_f - n_b)^2$ .

The  $\nu = 2$  QH state undergoes a phase transition from a compound state to a coherent state as the total density decreases or the densities are unbalanced, i.e., as the interlayer Coulomb interaction is increased over the intralayer Coulomb interaction. The stability of the  $\nu = 2$  QH state in the vicinity of the balanced configuration is quite similar to that of the  $\nu = 2/3$  state, and it can be regarded as a compound state at  $\nu = 1 + 1$ . However, when the total density becomes sufficiently small at  $n_t = 0.6 \times 10^{11} \text{ cm}^{-2}$ , we observe in Figs. 2 and 3 that the plateau width and the activation energy behave as those of the  $\nu = 1$  state which we identify as the coherent state. The reason why we have a coherent state at  $\nu = 2$  can be explained by considering the spin degree of freedom. In the  $\nu = 1$  state all electrons are in the *spin-up* states. It is natural to expect another coherent state with *spin-down* polarization above the  $\nu = 1$  state at  $\nu = 2$ . In this  $\nu = 2$  coherent state the total system is spin unpolarized. On the contrary, the  $\nu = 1 + 1$  compound state is fully spin polarized. This interpretation of the  $\nu = 2$  state is consistent with a recent inelastic light scattering experiment [14], where they observed a spin-polarized state in a high density sample and a spin-unpolarized state in a low density sample at  $\nu = 2$ .

In conclusion, by measuring the plateau width and the activation energy by continuously changing the electron density in each layer, we have revealed that the observed bilayer QH states ( $\nu = 2/3, 1$ , and  $2$ ) can be categorized into two distinctly different states. The  $\nu = 2/3$  state is a typical compound state with  $\nu = 1/3 + 1/3$  stabilized solely by the intralayer Coulomb interaction, whereas the  $\nu = 1$  state is a coherent state stabilized by the strong interlayer Coulomb interaction. The  $\nu = 2$  state shows a phase transition from the compound state to the coherent state as the interlayer Coulomb interaction becomes dominant. The appearance of such a  $\nu = 2$  coherent state is a consequence of the spin degree of freedom in the bilayer QH state.

We thank T. Saku (NTT) for growing the sample used in the present work, T. Nakajima for useful discussions, and N. Kumada for experimental support. Part of this work was done at the Laboratory for Electronic Intelligent Systems, RIEC, Tohoku University. Supports from a Grant-in-Aids for the Scientific Research from the Ministry of Education, Science, Sports and Culture (No. 08640438, No. 09244103, and No. 09244204), and from the Multi-disciplinary Science Foundation are acknowledged.

*Note added.*—After submission of this paper, we learned about the following theoretical papers on  $\nu = 2$  states: L. Zheng *et al.*, Phys. Rev. Lett. **78**, 2453 (1997); S. Das Sarma *et al.*, Phys. Rev. Lett. **78**, 917 (1997). We are grateful to Das Sarma for bringing them to our attention.

- 
- [1] A. H. MacDonald, P. M. Platzmann, and G. S. Boebinger, Phys. Rev. Lett. **65**, 775 (1990).
  - [2] S. He, S. Das Sarma, and X. C. Xie, Phys. Rev. B **47**, 4394 (1993).
  - [3] G. S. Boebinger, H. W. Jiang, L. N. Pfeiffer, and K. W. West, Phys. Rev. Lett. **64**, 1793 (1990).
  - [4] Y. W. Suen, L. W. Engel, M. B. Santos, M. Shayegan, and D. C. Tsui, Phys. Rev. Lett. **68**, 1379 (1992); J. P. Eisenstein, G. S. Boebinger, L. N. Pfeiffer, K. W. West, and Song He, Phys. Rev. Lett. **68**, 1383 (1992).
  - [5] Z. F. Ezawa and A. Iwazaki, Int. J. Mod. Phys. B **6**, 3205 (1992); Phys. Rev. B **47**, 7295 (1993); Phys. Rev. B **48**, 15 189 (1993).
  - [6] X. G. Wen and A. Zee, Phys. Rev. Lett. **69**, 1811 (1992).
  - [7] S. Q. Murphy, J. P. Eisenstein, G. S. Boebinger, L. N. Pfeiffer, and K. W. West, Phys. Rev. Lett. **72**, 728 (1994).
  - [8] Z. F. Ezawa, Phys. Rev. B **51**, 11 152 (1995); Phys. Rev. B **55**, 7771 (1997); Z. F. Ezawa and A. Iwazaki, Int. J. Mod. Phys. B **8**, 2111 (1994).
  - [9] K. Yang, K. Moon, L. Zheng, A. H. MacDonald, S. M. Girvin, D. Yoshioka, and S. C. Zhang, Phys. Rev. Lett. **72**, 732 (1994); K. Moon, H. Mori, K. Yang, S. M. Girvin, A. H. MacDonald, L. Zheng, D. Yoshioka, and S. C. Zhang, Phys. Rev. B **51**, 5138 (1995).
  - [10] A. Sawada, Z. F. Ezawa, H. Ohno, Y. Horikoshi, O. Sugie, S. Kishimoto, F. Matsukura, Y. Ohno, and M. Yasumoto, Solid State Commun. **103**, 447 (1997).
  - [11] By the coherent state we mean the Halperin  $\Psi_{mmm}$  state, upon which the IQC is expected to develop spontaneously.
  - [12] A. Usher, R. J. Nicholas, J. J. Harris, and C. T. Foxon, Phys. Rev. B **41**, 1129 (1990). The effective  $g$  factor for the excitation gap at  $\nu = 2$  is about half of that in this reference. The difference might come from the disorder and/or Coulomb interaction which depend on sample quality and geometry.
  - [13] R. B. Laughlin, Phys. Rev. Lett. **50**, 1395 (1983); B. I. Halperin, Helv. Phys. Acta **56**, 75 (1983); F. D. M. Haldane and E. H. Rezayi, Phys. Rev. Lett. **60**, 956 (1988).
  - [14] V. Pellegrini, A. Pinczuk, B. S. Dennis, A. S. Plaut, L. N. Pfeiffer, and K. W. West, Phys. Rev. Lett. **78**, 310 (1997).